High Temperature Materials and Processes, Vol. 10, No. 1, 1991

Structural Investigation of Amorphous RE_2AlH_x Alloys (RE = Pr, Nd, Sm, Gd, Tb and Dy; x = 4.0-6.5) by X-ray Diffraction

E. Matsubara*, Y. Waseda*, X-G. Li**, K. Aoki**, and T. Masumoto**

**Research Institute of Mineral Dressing and Metallurgy (SENKEN)*
Tohoku University, Sendai 980, Japan

***Institute for Materials Research*
Tohoku University, Sendai 980, Japan

(Received April 4, 1990; final form May 1, 1990).

CONTENTS

ABSTRACT

Structural study of amorphous ternary alloys of RE_2AlH_X (RE = Pr, Nd, Sm, Gd, Tb and Dy) produced by the hydrogen-induced amorphization method has been systematically investigated using conventional RDF analysis with X-rays. For comparison, similar structural studies were also carried out with respect to amorphous RE_2Al alloys (RE = Nd, Sm, Gd, Tb and Dy) produced by rapid quenching from the melt. It is clearly found that the distinct structural features of the amorphous RE_2AlH_X alloys are not reproduced by simple random mixing of the constituent elements.

INTRODUCTION

A large number of amorphous alloys have been produced, usually by rapid quenching from the melt or by vapor deposition at rates sufficient to bypass crystallization. The hydrogen-induced amorphization (hereafter referred to as HIA) method has received attention as an alternate route for synthesis of amorphous alloys, since Yeh, Samwer and Johnson /1/ reported in 1983 the formation of an amorphous alloy by a solid-state reaction of the compound Zr_3Rh with the $L1_2$ structure. On the other hand, amorphous rare earth (RE)-aluminum base alloys have been of considerable interest because of their particular magnetic and electronic properties /2/. The intermetallic compounds of RE_2Al, which have the C23-type structure, have recently been found to transform from a crystalline phase to an amorphous phase by the HIA method. However, their structural features have not yet been revealed.

The main purpose of this paper is to present our systematic X-ray diffraction study on amorphous RE_2AlH_X alloys (RE = Pr, Nd, Sm, Gd, Tb and Dy; x = 4.0-6.5), produced by the HIA method. For comparison, we will also describe the results of amorphous RE_2Al alloys (RE = Nd, Sm, Gd, Tb and Dy) produced by usual rapid quenching from the melt.

EXPERIMENTAL

Intermetallic compounds of RE_2Al (RE = Pr, Nd, Sm, Gd, Tb and Dy) were prepared from high purity materials, Pr (99.8%), Nd (99.9%), Sm (99.9%), Gd (99.9%), Tb (99.8%), Dy (99.8%) and Al (99.99%) by arc melting in a dry argon gas atmosphere. Ingots were homogenized at 1123 K for one week in an evacuated quartz tube and cut into small blocks for absorption of hydrogen. Amorphous RE_2AlH_X alloys were synthesized by exposing pulverized crystalline intermetallic compounds to high purity hydrogen gas (7N) of 1.5 MPa in a stainless steel reactor at temperatures between 300 and 673 K. The samples obtained show the spherical form with the size ranging from 30-80 μm in diameter. From the RE_2Al master alloys, amorphous RE_2Al ribbons of 0.2 mm thickness and 2 mm width were prepared by a single roller quenching apparatus. These ribbons were cut into small pieces of about 20 mm length, closely arranged on an aluminum frame of about 15 mm width and 10 mm height, and then sandwiched to a few layers thickness for the X-ray scattering measurements. It should be noted that amorphous Pr_2Al alloy was not obtained by the single-roller quenching apparatus employed in the present work. More details of the method for sample preparation are described elsewhere /3,4/.

An experimental apparatus and the procedures for obtaining the X-ray scattering intensity, corrections of measured intensity data and its Fourier analysis were almost identical to those employed in previous studies of the structure of various amorphous alloys /5,6/. These procedures are now well established and thus only salient points relevant to the present work are given below.

High intense X-ray beams produced by a rotating anode generator with an Mo target of 50 kV and 190 mA were monochromated by a Ge 111 flat single crystal in the incident beam. The sample was maintained in dry helium gas during the course of the experiments in order to protect against sample oxidation. The intensity profiles were measured in the wave vector range of $Q = 4\pi \sin\Theta/\lambda$ from 9 to 153 nm^{-1}, where λ is the wavelength and 2Θ is the angle between the incident and diffracted X-rays. A fixed-count mode was applied and at least 20,000 counts were collected at every measured point so that the statistical counting error was less than $\pm 0.5\%$.

In this work, the observed intensity data at small Q values, less than 9 nm^{-1}, have been smoothly extrapolated to the value of $Q = 0$ nm^{-1}. The effect of the extrapolation and the truncation up to $Q = 153$ nm^{-1} is known not to give a critical contribution in the

calculation of the radial distribution function (RDF) by the Fourier transformation /7/. The RDF can be estimated from the so-called interference function $Qi(Q)$ for disordered systems including more than two kinds of atoms using the following equations /6,8/.

$$4\pi r^2\rho(r) = 4\pi r^2\rho_o + \int_0^{Q_{max}} Qi(Q)\sin(Qr)\,dQ \quad (1)$$

$$Qi(Q) = [I_{eu}^{coh}(Q) - \langle f^2\rangle + \langle f\rangle^2] / \langle f\rangle^2 \quad (2)$$

$$\langle f\rangle = \sum_{j=1}^{n} c_j f_j, \quad \langle f^2\rangle = \sum_{j=1}^{n} c_i f_i^2 \quad (3)$$

where $I_{eu}^{coh}(Q)$ is the coherent X-ray scattering intensity per atom in electron units, which is directly obtained from measured intensity data, and Q_{max} is the maximum Q-value measured, 153 nm^{-1} in the present case. The quantities c_j, $\rho(r)$ and ρ_o are the concentration of the jth element, the average radial density function and the average number density of atoms, respectively. The quantity f_j is the X-ray atomic scattering factor including the anomalous dispersion terms of the jth element and is taken from the International Tables for X-ray Crystallography /9/.

RESULTS AND DISCUSSION

Figure 1 shows the interference function $Qi(Q)$ of amorphous RE_2AlH_X alloys produced by the HIA

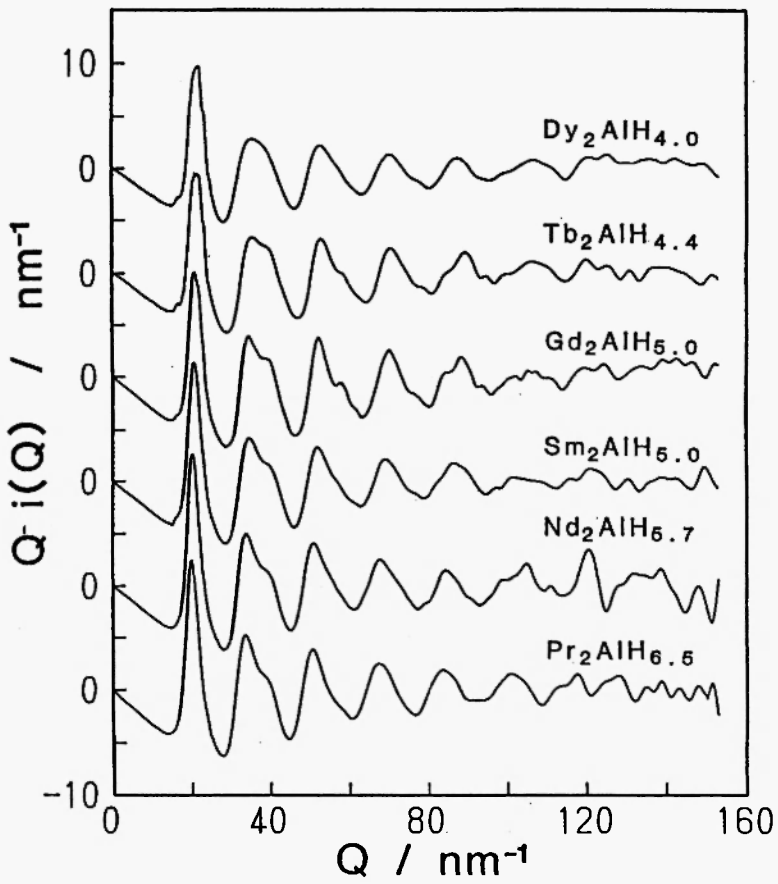

Fig. 1: Interference functions $Qi(Q)$ of amorphous RE_2AlH_X alloys produced by the HIA method.

method. For comparison, the interference functions of five amorphous RE_2Al alloys obtained by rapid quenching from the melt are also illustrated in Fig. 2. Note that the vertical scale is different in these two figures. In addition, aluminum and hydrogen atoms have considerably small scattering ability compared to those of rare earth atoms. Thus, measured intensity data mainly arises from the contribution of rare earth atoms and the RDF information may be reasonably approximated by the distribution of rare earth atoms in both amorphous RE_2AlH_X and RE_2Al alloys.

The profiles of these interference functions are classified into a typical non-crystalline structure characterized by the relatively sharp first peak, and the second peak with a shoulder on the high-Q region. However, the first peak height of the amorphous alloys produced by hydrogenation is rather distinct compared with the amorphous RE_2Al alloys obtained by the conventional method and the second peak shoulder of the amorphous RE_2Al alloys is obscure. In addition, as easily seen from Fig. 1, the oscillations in the interference function of the amorphous RE_2AlH_X alloys still remain in the higher-Q region, where the oscillations are well reduced in various amorphous alloys produced by the conventional methods, including the amorphous RE_2Al alloys, and such a character is rather close to the cases of semiconducting liquids or oxides glasses /10/. This qualitatively implies a certain short-range order, indicating the presence of species with definite lengths and angular relations remaining in the amorphous RE_2AlH_X alloys.

The radial distribution functions (RDFs) of the amorphous RE_2AlH_X and RE_2Al alloys calculated from the $Qi(Q)$ data using Eq. (1) with the measured density

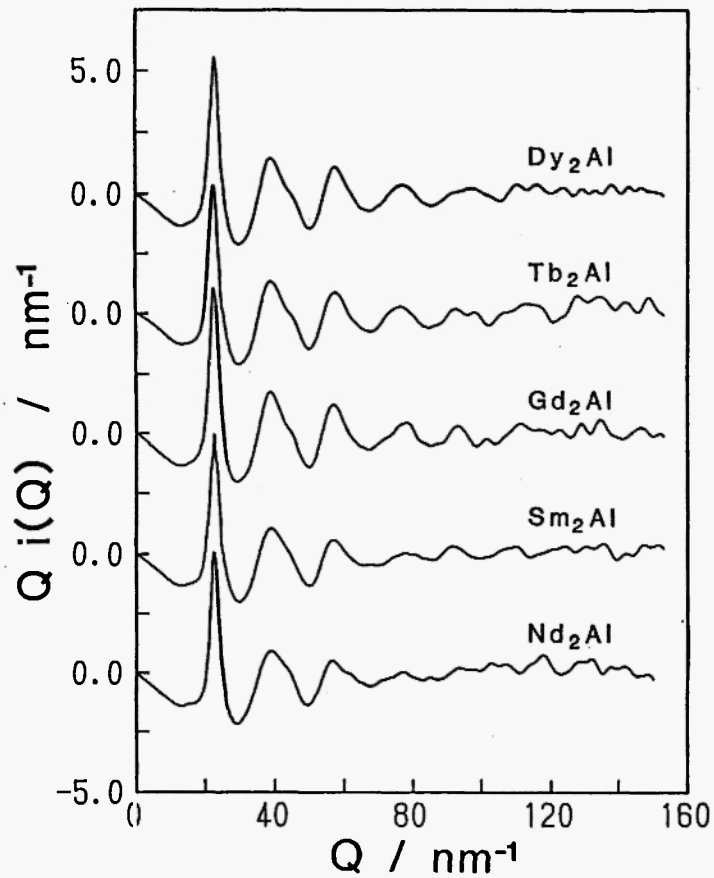

Fig. 2: Interference functions $Qi(Q)$ of amorphous RE_2Al alloys produced by rapid quenching from the melt.

data listed in Table 1 are given in Figs. 3 and 4. In all cases, the spurious ripples in the small r region are sufficiently reduced, which is consistent with the physical property that the RDF is essentially zero inside the atomic diameter. For convenience of discussion, a comparison of the RDF data is given in Fig. 5 in the same vertical scale, using the results of a Tb-Al case together with the near neighbor distances estimated from the Goldschmidt radii /11/ and from the crystalline hydride phase of TbH_2 /12/.

In terms of the nearest neighboring distances computed from the Goldschmidt radii (Tb: 0.177 nm, Al: 0.143 nm), it is found that the maximum and the shoulder at the lower-r side of the first peak in the amorphous Tb_2Al alloy of Fig. 5 corresponds to Tb-Tb and Tb-Al pairs, respectively. As mentioned above, the contribution of the Al-Al pairs to the RDF is about 1% of that for the Tb-Al pairs in the Tb_2Al alloy. Thus, by fitting this particular peak and shoulder with two Gaussian curves and by ascribing them to the Tb-Tb and

TABLE 1
DENSITIES OF AMORPHOUS RE_2AlH_X AND RE_2Al ALLOYS MEASURED BY ARCHIMEDES' METHOD WITH TOLUENE

Sample	Density (Mg m^{-3})
$Pr_2AlH_{6.5}$	4.81
$Nd_2AlH_{5.7}$	5.10
$Sm_2AlH_{5.0}$	5.44
$Gd_2AlH_{5.0}$	5.78
$Tb_2AlH_{4.4}$	6.11
$Dy_2AlH_{4.1}$	6.26
Nd_2Al	5.84
Sm_2Al	5.98
Gd_2Al	6.66
Tb_2Al	7.19
Dy_2Al	7.36

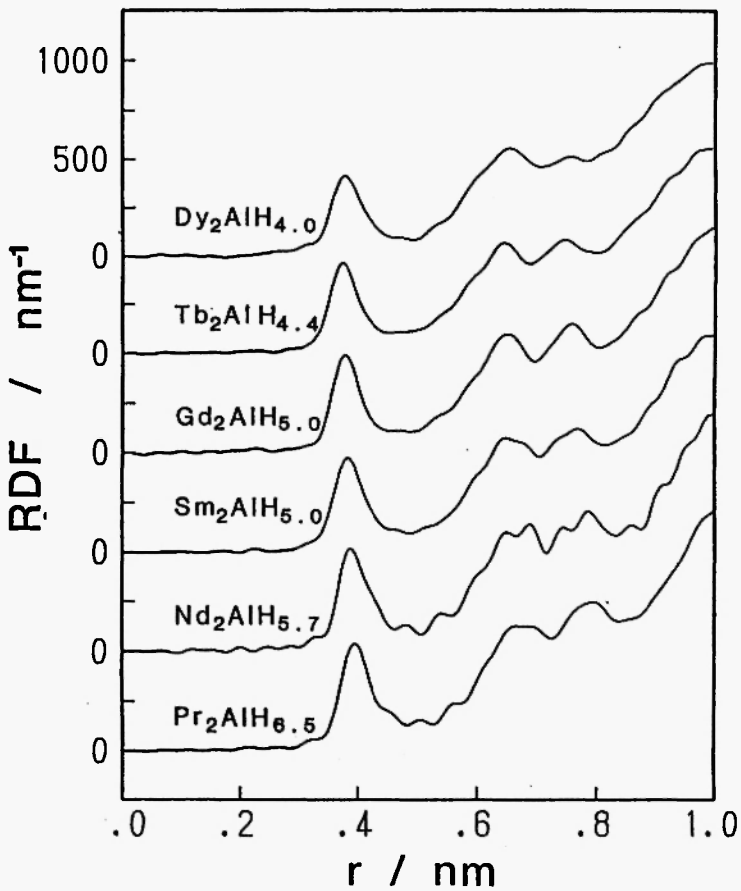

Fig. 3: Radial distribution functions of amorphous RE_2AlH_X alloys produced by the HIA method.

Tb-Al pairs, the coordination numbers around Tb at the nearest neighboring distances are determined to be 6.1 for Tb at 0.325 nm and 3.2 for Al at 0.312 nm. These coordination numbers are proportional to the atomic fractions, which implies that there does not appear to be any tendency of either segregation or compound formation in the amorphous Tb_2Al alloy.

On the other hand, the first peak position of amorphous $Tb_2AlH_{4.4}$ clearly shifts towards the longer distance, which is rather coincident with the nearest Tb-Tb distance in crystalline hydride of TbH_2. Such coincidence is also detected in the longer distance region with respect to the Tb-Tb correlation distances.

The first peak in the RDF of the amorphous $Tb_2AlH_{4.4}$ alloy appears to be relatively sharp and almost resolved, although the subsequent oscillations of the RDF decay rapidly and no structurally significant deviation from the average value of $4\pi r^2\rho_0$ is detected at $r \geq 1.0$ nm. This type of atomic configuration of a non-crystalline system corresponds to distinct local nearest neighbor correlations, as seen in semiconducting liquids (Te and Se) and oxide glasses, accompanied by a complete loss of correlation between such units at larger distances /8,10/. For this reason, in the amorphous RE_2AlH_X alloys, the definite clusters formed by metallic elements are quite feasible as a local ordering unit, which is one of the elemental structural units in the crystalline rare earth metal hydrides such as TbH_2. This contrasts to the usual near neighbor correlations observed in various amorphous alloys produced by rapid quenching from the melt, including the amorphous RE_2Al alloys.

These observations, in both structural functions of $Qi(Q)$ and RDFs for the amorphous RE_2AlH_X alloys,

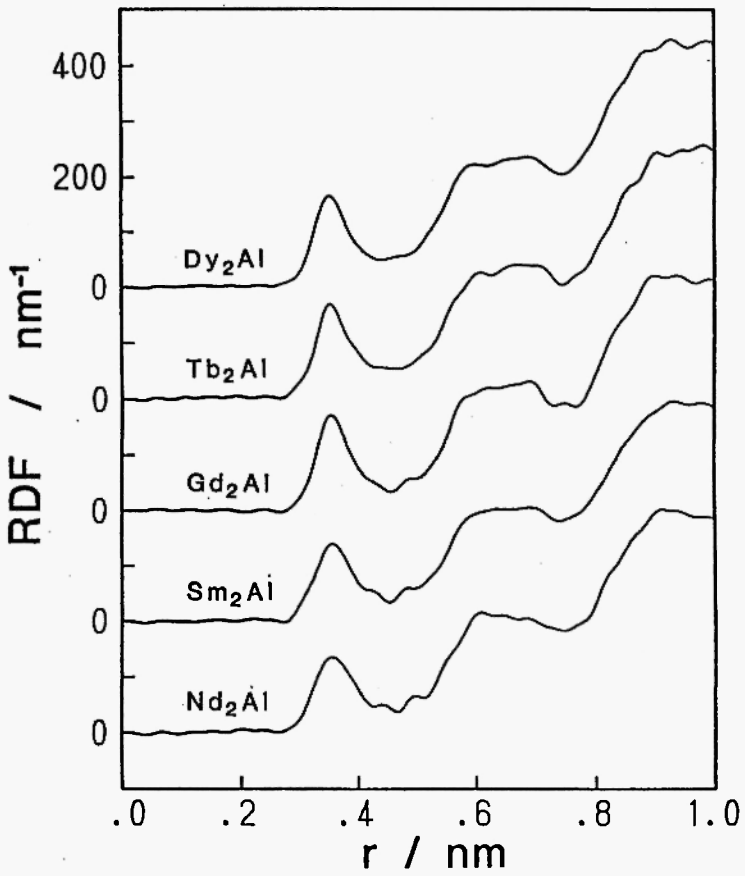

Fig. 4: Radial distribution functions of amorphous RE_2Al alloys produced by rapid quenching from the melt.

are essentially similar to the previous works on amorphous $CeFe_2H_3$ and $GdFe_2H_3$ alloys /13/ or $ZrIn_3H_3$ and $ZrAl_3H_3$ alloys /14/ produced by the HIA method. However, there are six possible atomic pairs in each system because three elements are involved in the present samples. Thus further experimentation, particularly to determine the fine structure such as partial RDFs or the environmental RDFs of the individual constituent atoms in these amorphous alloys, is strongly desirable in order to quantitatively specify the origin of the characteristic structural features presently observed, even if we consider the fact that the scattering factors of hydrogen and aluminum are much less than those of rare earth elements.

To summarize the results in the present work, amorphous RE_2AlH_X alloys produced by hydrogenation of the pulverized intermetallic compounds of RE_2Al with the C23 structure in pressurized pure hydrogen gas at relatively low temperature show the distinctively different structural features characterized by the almost resolved first peak in RDF which should be attributed to the definite clusters formed mainly by rare earth atoms.

ACKNOWLEDGEMENTS

The authors (EM and YM) would like to thank the Light Metal Educational Foundation Inc. for its financial support.

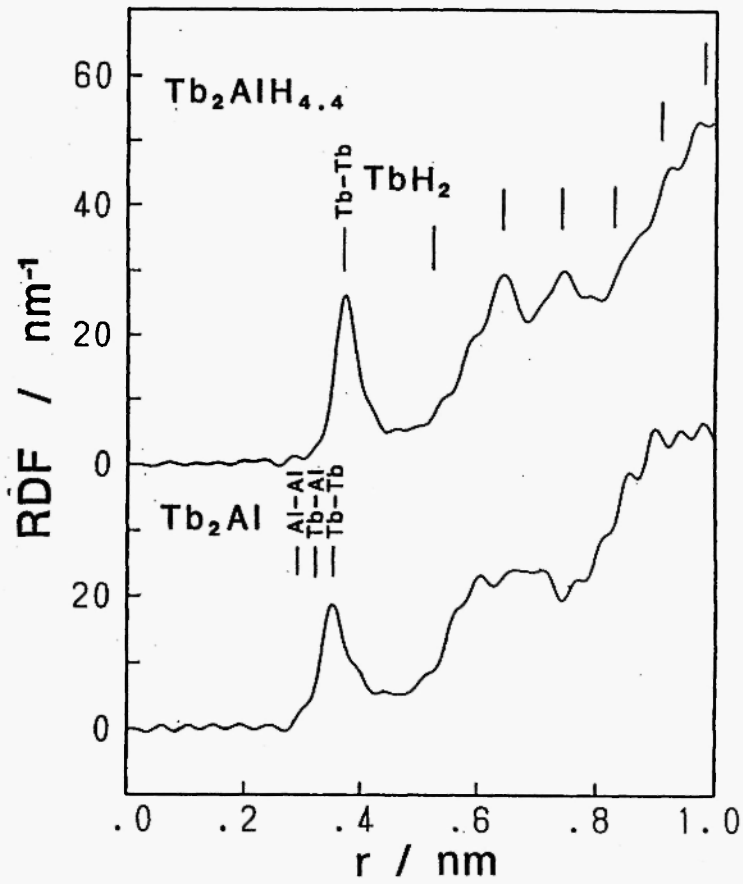

Fig. 5: A comparison of the RDF data of amorphous $Tb_2AlH_{4.4}$ alloy with that of amorphous Tb_2Al alloy. Bars indicate positions of some pairs calculated from the Goldschmidt radii and from a crystalline hydride phase of TbH_2. The RDF values should be read by the factor of 10.

REFERENCES

1. Yeh, X.L., Samwer, K. and Johnson, W.L., *Appl. Phys. Lett.*, **42**, 242 (1983).
2. See, for example, Shirakawa, K., Aoki, K. and Masumoto, T., *J. Non-Cryst. Solids*, **61/62**, 1371 (1984).
3. Aoki K., Shirakawa K. and Masumoto T., *Sci. Rep. Res. Inst.*, Tohoku Univ., **32A**, 231 (1985).
4. Inoue, A., Matsuzaki, K., Ogashima, T. and Masumoto T., *J. Mater. Sci.*, **22**, 2063 (1987).
5. Matsubara E., Harada, K., Waseda, Y., Chen, H.S., Inoue, A. and Masumoto T., *J. Mater. Sci.*, **23**, 753 (1988).
6. Wagner, C.N.J., *J. Non-Cryst. Solids*, **31**, 1 (1978).
7. Furukawa K., *Rep. Progr. Phys.*, **25**, 395 (1962).
8. Waseda, Y., "The Structure of Non-Crystalline Materials," McGraw-Hill, New York, 1980.
9. "International Tables for X-ray Crystallography, Vol. IV," The Kynoch Press, Birmingham, 1974.
10. Egelstaff, P.A., Page, D.I. and Powles, J.G., *Mol. Phys.*, **20**, 881 (1971).
11. Goldschmidt, V.M., "Geochemistry," Oxford, London, 1954.
12. Pearson, W.B., "Handbook of Lattice Spacing and Structure of Metals," Pergamon Press, New York, 1967.
13. Matsubara, E., Ohzora, Y., Waseda, Y., Aoki, A., Fukamichi, K. and Masumoto T., *Zeit. für Naturforsch.*, **42a**, 582 (1987).
14. Matsubara, E., Waseda, Y., Li, X-G., Aoki, K. and Masumoto, T., *J. Mater. Sci. Letters*, **9**, 1017 (1990).